YAP1, the nuclear target of Hippo signaling, stimulates heart growth through cardiomyocyte proliferation but not hypertrophy

Alexander von Gise[a,b,1], Zhiqiang Lin[a,1], Karin Schlegelmilch[c,d,e,f], Leah B. Honor[a], Gina M. Pan[a], Jessica N. Buck[a], Qing Ma[a], Takahiro Ishiwata[g], Bin Zhou[a,h], Fernando D. Camargo[c,e,f], and William T. Pu[a,f,2]

[a]Department of Cardiology and [c]Stem Cell Program, Children's Hospital Boston, Boston, MA 02115; [b]Department of Neonatology, Charité University Medical Center, 10117 Berlin, Germany; [d]Institute for Chemistry/Biochemistry, Freie Universität Berlin, 14195 Berlin, Germany; [e]Department of Stem Cell and Regenerative Biology, Harvard University, Cambridge, MA 02138; [f]Harvard Stem Cell Institute, Cambridge, MA 02138; [g]Division of Cardiology, Department of Internal Medicine, University of Utah, Salt Lake City, UT 84132; and [h]Key Laboratory of Nutrition and Metabolism, Institute for Nutritional Sciences, Shanghai Institutes for Biological Sciences, Chinese Academy of Sciences, Shanghai 200031, China

Edited* by Jonathan G. Seidman, Harvard Medical School, Boston, MA, and approved December 27, 2011 (received for review October 3, 2011)

Heart growth is tightly controlled so that the heart reaches a predetermined size. Fetal heart growth occurs through cardiomyocyte proliferation, whereas postnatal heart growth involves primarily physiological cardiomyocyte hypertrophy. The Hippo kinase cascade is an important regulator of organ growth. A major target of this kinase cascade is YAP1, a transcriptional coactivator that is inactivated by Hippo kinase activity. Here, we used both genetic gain and loss of *Yap1* function to investigate its role in regulating proliferative and physiologic hypertrophic heart growth. Fetal *Yap1* inactivation caused marked, lethal myocardial hypoplasia and decreased cardiomyocyte proliferation, whereas fetal activation of YAP1 stimulated cardiomyocyte proliferation. Enhanced proliferation was particularly dramatic in trabecular cardiomyocytes that normally exit from the cell cycle. Remarkably, YAP1 activation was sufficient to stimulate proliferation of postnatal cardiomyocytes, both in culture and in the intact heart. A dominant negative peptide that blocked YAP1 binding to TEAD transcription factors inhibited YAP1 proliferative activity, indicating that this activity requires YAP1–TEAD interaction. Although Yap1 was a critical regulator of cardiomyocyte proliferation, it did not influence physiological hypertrophic growth of cardiomyocytes, because postnatal *Yap1* gain or loss of function did not significantly alter cardiomyocyte size. These studies demonstrate that *Yap1* is a crucial regulator of cardiomyocyte proliferation, cardiac morphogenesis, and myocardial trabeculation. Activation of *Yap1* in postnatal cardiomyocytes may be a useful strategy to stimulate cardiomyocyte expansion in therapeutic myocardial regeneration.

heart development | physiological hypertrophy

Between the early heart tube stage and adulthood, the murine heart increases by >300-fold in mass (Fig. S1) (1). The ~18-fold increase in mass achieved during fetal life occurs mainly through cardiomyocyte proliferation, whereas the remaining ~18-fold growth achieved postnatally largely involves increased cardiomyocyte size (physiological hypertrophy), plus expansion of nonmyocyte populations. Growth of the heart is precisely regulated so that there is little variability in the final size of the adult heart. Derangements of these regulatory pathways likely contribute to congenital heart malformations, the leading form of major birth defect. Moreover, understanding of these pathways will be highly relevant for regenerative approaches to postnatal heart disease.

The Hippo signaling cascade was discovered in *Drosophila* as a potent mechanism that regulates cell proliferation and organ size (2, 3). The core kinases of this signaling pathway, Hippo (Hpo) and Warts (Wts), and their regulatory subunits Salvador (Sav) and Mats, phosphorylate Yorkie (Yki) (4–7). In the absence of phosphorylation by the Hpo kinases cascade, Yki coactivates transcription in conjunction with specific transcription factors, such as the TEAD family transcription factor Scalloped (Sd), stimulating organ growth by increasing cell proliferation and reducing apoptosis (8, 9). Incompletely understood upstream molecular signals activate the Hpo kinase cascade, leading to Yki phosphorylation, nuclear export, and reduced organ growth. The core of the Hippo pathway is highly conserved in mammals, where *Mst1/2*, *Sav1*, *Lats1/2*, *Yap1*, and *Tead1-4* are the orthologs of Hpo, Sav, Wts, Yki, and Sd, respectively (3). *Yap1* gain and loss of function in liver and skin suggest that *Yap1* plays an important role in mammalian organ size regulation, as in *Drosophila* (10–12).

In this study, we investigated the function of *Yap1* in regulating heart growth. *Yap1* loss of function impaired cardiomyocyte proliferation and caused lethal myocardial hypoplasia. Meanwhile, *Yap1* gain of function enhanced cell-cycle activity in cardiomyocytes both in vitro and in intact fetal and infant hearts. However, *Yap1* gain and loss of function did not substantially alter cell size, indicating that *Yap1* influences organ size primarily by regulating proliferation. Collectively, our data demonstrate that *Yap1* is a powerful regulator of cardiomyocyte proliferation.

DEVELOPMENTAL BIOLOGY

Results

YAP1 Expression in Fetal and Postnatal Heart. We measured YAP1 expression at different stages of heart development. YAP1 protein was robustly detected in neonatal and juvenile mouse heart and declined with age, so that it was nearly undetectable by 12 wk of age (Fig. S2*A*). To distinguish expression in myocytes compared with nonmyocytes, we dissociated fetal, neonatal, and adult hearts and separated cells into myocyte and nonmyocyte fractions. By Western blotting, YAP1 was detected in both myocytes and nonmyocytes, with predominantly cardiomyocyte expression in fetal heart (Fig. S2*B*). In neonatal and 1.5-mo-old heart, expression levels in cardiomyocytes and nonmyocytes were comparable (Fig. S2*B*).

Fetal Cardiomyocyte-Restricted Loss of *Yap1* Causes Lethal Cardiac Hypoplasia. To test the hypothesis that *Yap1* is required for fetal cardiomyocyte proliferation, we inactivated a conditional *Yap1* allele ($Yap1^{flox}$) specifically in cardiomyocytes early in heart development using Tnnt2–Cre (13). To measure the extent of *Yap1* inactivation, we used FACS to isolate pure populations of cardiomyocytes from $Yap1^{fl/+}$::Tnnt2–Cre::$Rosa26^{mTmG/+}$ (*Yap1* heterozygous control) or $Yap1^{fl/fl}$::Tnnt2–Cre::$Rosa26^{mTmG/+}$

Author contributions: A.v.G., Z.L., and W.T.P. designed research; A.v.G., Z.L., K.S., L.B.H., G.M.P., J.N.B., Q.M., and T.I. performed research; K.S. and F.D.C. contributed new reagents/analytic tools; A.v.G., Z.L., L.B.H., G.M.P., J.N.B., Q.M., and W.T.P. analyzed data; and A.v.G., Z.L., and W.T.P. wrote the paper.

The authors declare no conflict of interest.

*This Direct Submission article had a prearranged editor.

Data deposition: The data reported in this paper have been deposited in the Gene Expression Omnibus (GEO) database, www.ncbi.nlm.nih.gov/geo (accession no. GSE33019).

[1]A.v.G. and Z.L. contributed equally to this work.

[2]To whom correspondence should be addressed. E-mail: wpu@enders.tch.harvard.edu.

This article contains supporting information online at www.pnas.org/lookup/suppl/doi:10.1073/pnas.1116136109/-/DCSupplemental.

(*Yap1* mutant) heart at embryonic day (E) 12.5. In these embryos, Tnnt2–Cre activated membrane-localized GFP (mGFP) from the Cre-activated Rosa26^{mTmG} reporter and inactivated the conditional *Yap1* allele specifically in cardiomyocytes. By quantitative RT-PCR (qRT-PCR), *Yap1* transcripts were depleted by >95% at E12.5 in mutant compared with heterozygous control cardiomyocytes (Fig. 1*A*), confirming effective gene inactivation.

Yap1$^{fl/fl}$::Tnnt2–Cre (abbreviated Yap1^{Tnnt2}) embryos were present at a sub-Mendelian ratio by E12.5 and were not recovered beyond E16.5. The embryos displayed peripheral edema and pericardial effusion, consistent with heart failure (Fig. 1*B* and Fig. S3*A*). Overall cardiac patterning was preserved, but ventricular chamber size was severely reduced (Fig. 1*C* and Fig. S3*B*). In some cases, the hypoplasia affected both ventricles equally, whereas in other cases the left ventricle was more severely affected. Histological sectioning demonstrated a four-chambered heart with two atrioventricular and two outflow tract valves (Fig. 1*D* and Fig. S3*C*). The myocardium was markedly hypoplastic (Fig. 1*D*). Expression of MLC2A (MGI:MYL7) and MLC2V (MGI:MYL2), markers of atria and ventricular chamber specification, was unperturbed (Fig. S3*D*), indicating normal chamber specification. Rare survivors to E16.5 had ventricular septal defects (Fig. S3*C*).

To investigate the cellular mechanism underlying the myocardial hypoplasia, we performed immunostaining for markers of proliferation and apoptosis. Staining for histone H3 phosphorylated on serine 10 (pH3), a marker of M phase of the cell cycle, showed substantially reduced cardiomyocyte proliferation. Quantitative analysis showed that the fraction of cardiomyocytes positive for pH3 was reduced by twofold ($P < 0.05$; Fig. 1 *E* and *F*). This result was confirmed by analysis of cardiomyocyte uptake of 5-ethynyl-2'-deoxyuridine (EdU), a nucleotide analog that labels cells passing through S phase. EdU$^+$ cardiomyocytes were reduced by twofold in Yap1^{Tnnt2} mutant heart ($P < 0.05$; Fig. 1 *G* and *H*). Although YAP1 regulates apoptosis in other settings (14), apoptosis was not elevated in Yap1^{Tnnt2} cardiomyocytes, as assessed by TUNEL staining (Fig. S3*E*). Collectively, these data indicate that *Yap1* is essential for fetal cardiomyocyte proliferation.

To confirm that reduced cardiomyocyte proliferation led to decreased cardiomyocyte number, we used FACS to quantitate cardiomyocyte number in dissociated fetal hearts (Fig. S3 *F* and *G*). We took advantage of the Rosa26^{mTmG} (15) Cre reporter allele, in which Cre activity switches off baseline mRFP (membrane-bound RFP) and activates mGFP. GFP$^+$ cardiomyocyte number was reduced in Yap1$^{fl/fl}$::Tnnt2–Cre::Rosa26$^{mTmG/+}$ mutants compared with Yap1$^{fl/+}$::Tnnt2–Cre::Rosa26$^{mTmG/+}$ heterozygous controls. On the other hand, cardiomyocyte size, as measured by FACS forward scatter, did not differ between groups, suggesting that *Yap1* is not required for fetal cardiomyocyte size regulation (Fig. S3*H*). Collectively, these data indicate that *Yap1* is required to promote normal cardiomyocyte proliferation in the fetal heart.

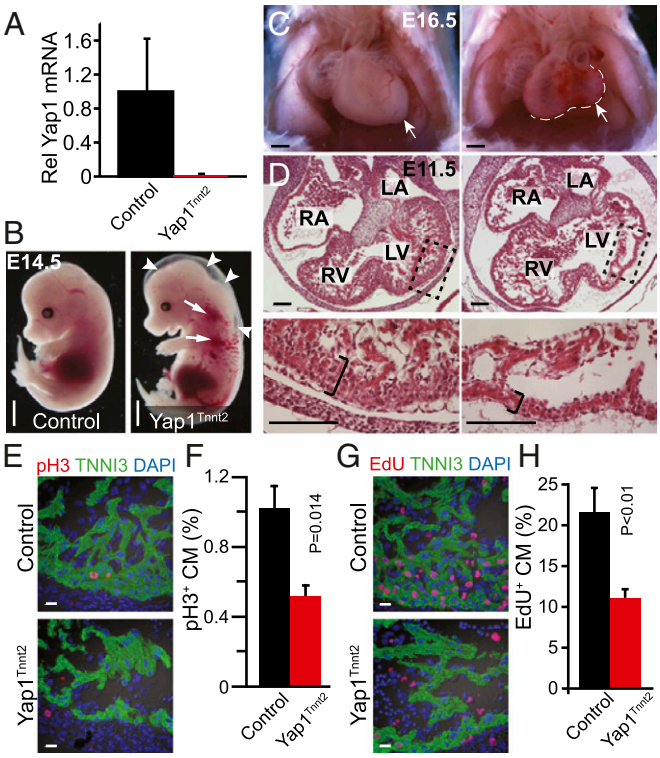

Fig. 1. Fetal cardiomyocyte-restricted inactivation of YAP1. (*A*) YAP1 mRNA levels in control (Yap1$^{fl/+}$::Tnnt2–Cre::Rosa26$^{mTmG/+}$) and Yap1^{Tnnt2} (Yap1$^{fl/fl}$::Tnnt2–Cre::Rosa26$^{mTmG/+}$) mutant cardiomyocytes, isolated at E12.5 by FACS for GFP. (*B*) *Hydrops fetalis* and peripheral hemorrhage in mutant embryo at E13.5. (Scale bar: 500 μm.) (*C*) Whole-mount image of E16.5 embryos after removal of the ventral chest wall, showing severe hypoplasia of mutant hearts. Hypoplasia was more severe in the left ventricle. For clarity, the white line indicates the edge of the heart. (Scale bar: 500 μm.) (*D*) Histological sections of E11.5 hearts. Magnifications show dramatic hypoplasia of compact myocardium in mutants (black brackets). (Scale bar: 100 μm.) (*E* and *F*) Reduced pH3 immunoreactivity in Yap1^{Tnnt2} mutant hearts. $n = 3$. (Scale bar in *E*: 10 μm.) (*G* and *H*) Reduced EdU staining in Yap1^{Tnnt2} mutant hearts. $n = 3$. (Scale bar: 10 μm.)

Cardiomyocyte Hypertrophic Growth Does Not Require *Yap1*. The fetal heart primarily grows through cardiomyocyte proliferation, but by postnatal day (P) 4, cardiomyocytes stop increasing in number and postnatal heart growth occurs by increased cardiomyocyte size (physiological hypertrophy) (16). Loss of *Yap1* in the fetal heart impaired cardiomyocyte proliferation but did not alter size. Therefore, we hypothesized that Yap1 is dispensable for physiological cardiomyocyte hypertrophy.

To test this hypothesis, we asked whether loss of *Yap1* has a cell-autonomous effect on postnatal cardiomyocyte growth. We sought to inactivate *Yap1* postnatally in a small fraction of cardiomyocytes, to avoid potentially triggering secondary effects that may result from widespread myocardial *Yap1* inactivation. A previous report indicated that retro-orbital administration of adenovirus to newborn pups leads to mosaic cardiomyocyte gene transfer (17). Retro-orbital delivery of Ad:Tnnt2–Cre to Yap1$^{fl/fl}$::Rosa26$^{mTmG/mTmG}$ pups activated the Cre-dependent mGFP reporter (and inactivated the baseline mRFP reporter) in a small fraction of cardiomyocytes, confirming that this technique is an effective means to achieve mosaic Cre-mediated recombination in the heart (Fig. 2*A*). We did not observe GFP expression outside of the heart.

To investigate the cell-autonomous role of *Yap1* in postnatal cardiomyocyte growth, we delivered Ad:Tnnt2–Cre to Yap1$^{fl/fl}$::Rosa26$^{mTmG/mTmG}$ pups at 3 d of life. At 4–6 wk of life, we compared the size of GFP$^+$ (*Yap1*-deficient) and GFP$^-$ (control) cardiomyocytes. In tissue sections, the cross-sectional areas of GFP$^+$ and GFP$^-$ cardiomyocytes did not differ significantly (Fig. 2*B*). Likewise, in dissociated cardiomyocyte preparations, cardiomyocyte projected area was not significantly altered (Fig. 2*C*). Thus, we conclude that *Yap1* is not required in a cell-autonomous manner for physiological cardiac hypertrophy.

Cardiomyocytes also increase in size in response to biomechanical stress, a process known as pathological hypertrophy. To determine whether YAP1 is essential for pathological hypertrophy, we performed ascending aortic constriction (AAC) on adult mice with mosaic inactivation of *Yap1*. The cross-sectional area of GFP$^-$ control cardiomyocytes was larger in AAC compared with unoperated hearts, consistent with activation of the hypertrophic response (Fig. S4). GFP$^+$ mutant cardiomyocytes were not significantly different in size compared with GFP$^-$ cardiomyocytes in either unoperated or AAC hearts (Fig. S4). Thus, YAP1 was dispensable for pathological cardiomyocyte hypertrophy.

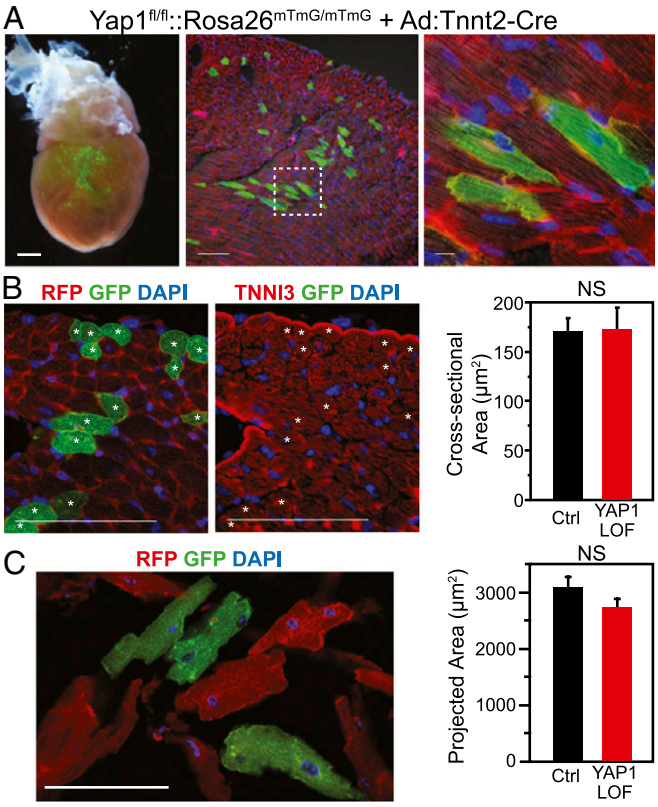

Fig. 2. YAP1 is not cell autonomously required for postnatal hypertrophic cardiomyocyte growth. (*A*) Mosaic Cre-mediated recombination after retro-orbital delivery of Ad:Tnnt2–Cre to P3 neonatal Yap1$^{fl/fl}$::Rosa26$^{mTmG/mTmG}$ mice. Boxed area is magnified in the *Right* panel. [Scale bars (from left): 500, 100, 10 μm.] (*B* and *C*) Hearts were examined at 4 wk (*B*) or 6 wk (*C*). Sizes of YAP1-deficient (mGFP$^+$ and mRFP$^-$) and control (mGFP$^-$ and mRFP$^+$) cardiomyocytes were measured in histological sections (cross-sectional area, *B*) or in dissociated preparations (projected area, *C*). No significant difference was detected between groups (NS; n = 4). (Scale bars: 100 μm.)

***Yap1* Gain of Function Stimulates Proliferation of Cultured Cardiomyocytes.** Given the essential role of *Yap1* in sustaining normal cardiomyocyte proliferation, we next asked whether increased *Yap1* is sufficient to drive cardiomyocyte proliferation. We developed an adenoviral vector to express activated YAP1 with an N-terminal triple FLAG epitope (Ad:FLAG–aYap1), where "activated YAP1" contained a serine 127 to alanine substitution that blocked Hippo pathway-mediated YAP1 inactivation (18). We confirmed expression in cultured neonatal rat cardiomyocytes (Fig. S5*A*). We used this tool to ask whether YAP1 gain of function enhances proliferation of fetal cardiomyocytes, which are normally actively proliferating. We transduced wild-type E16.5 fetal rat cardiomyocytes with Ad:FLAG–aYap1 or control (LacZ-expressing adenovirus, Ad:LacZ) adenovirus and measured the fraction of cells undergoing DNA synthesis [5′-bromodeoxyuridine (BrdU) uptake and mitosis (pH3 staining)]. Activated YAP1 significantly increased both measures of cardiomyocyte cell-cycle activity (Fig. S5*B*). Consistent with active fetal cardiomyocyte proliferation, the number of cardiomyocytes after 2 d of culture was greater in the activated YAP1 group compared with controls (Fig. S5*B*).

Having established that activated YAP1 was sufficient to stimulate proliferation of cardiomyocytes that were already actively engaged in the cell cycle, we next investigated whether *Yap1* gain of function could sustain proliferation in postnatal cardiomyocytes, which normally exit the cell cycle. Prior studies demonstrated that rat cardiomyocytes cease increasing in number by P4, although DNA synthesis and karyokinesis were detected above background levels for another 1–2 wk (16). Therefore, we prepared cardiomyocyte cultures from P4 neonatal rats. As expected, control neonatal rat ventricular cardiomyocytes treated with LacZ adenovirus rarely stained for pH3 or Aurora B, markers of M phase and cytokinesis, respectively, confirming that nearly all neonatal cardiomyocytes had exited the cell cycle (Fig. 3*A*). A small fraction (2%) of control neonatal cardiomyocytes were labeled with BrdU, consistent with low-level, persistent DNA synthesis activity (Fig. 3*A*). In contrast to control neonatal cardiomyocytes , aYAP1 neonatal cardiomyocytes exhibited far greater cell-cycle activity, with labeling indexes of 31%, 2.7%, and 2.1% for BrdU, pH3, and AuroraB, respectively (Fig. 3*A*). aYAP1 neonatal cardiomyocytes were observed at all stages of the cell cycle (Fig. S5*C*). Sequential imaging of the same fields over time demonstrated completion of cytokinesis in a subset of aYAP1-expressing but not control cardiomyocytes (Fig. 3*B* and Fig. S5*D*). We detected cell division events in 0/366 control cells, 0/267 LacZ cells, and 8/566 aYAP1 cells (P = 0.015; Fig. 3*B*). However, there was ongoing apoptosis in these cultures, which was reduced, but not eliminated, with FLAG–aYap1 expression (Fig. S5 *E* and *F*). As a result, there was an overall decline in cardiomyocyte number over the course of the experiment, although this decline was least in the aYAP1 group as a result of both increased proliferation and reduced apoptosis (Fig. S5*G*). Collectively, these data indicate that activated YAP1 continues to drive the cell cycle in postnatal cardiomyocytes, which normally have very little cell-cycle activity.

Activated Yap1 Stimulated Fetal Cardiomyocyte Proliferation in Vivo. Next, we asked whether YAP1 gain of function stimulates cardiomyocyte proliferation in intact fetal heart. We used a reported transgene (TetO–aYap1) (10) that expresses activated YAP1 (YAP1–[S127A]) from a doxycycline (Dox)-dependent promoter. In Tnnt2–Cre::Rosa26$^{fs\text{-}rtTA}$::TetO-aYap1 (abbreviated Yap1^{GOF}) mice, Dox induced expression of activated YAP1 selectively in cardiomyocytes (Fig. S6 *A* and *B*). Administration of Dox to YAP1^{GOF} fetuses starting at E8.5 resulted in fetal demise by E15.5. At E12.5, mutant fetuses exhibited peripheral hemorrhage, hepatic congestion, and cardiomegaly (Fig. S6*C*). Histological examination revealed dramatic myocardial overgrowth with moderate thickening of the compact myocardium and marked expansion of the trabecular myocardium, causing near chamber obliteration (Fig. 4*A*, arrowheads).

To evaluate the cellular mechanism for myocardial expansion, we performed immunostaining for proliferation markers. Cardiomyocyte proliferation was significantly increased in Yap1^{GOF}

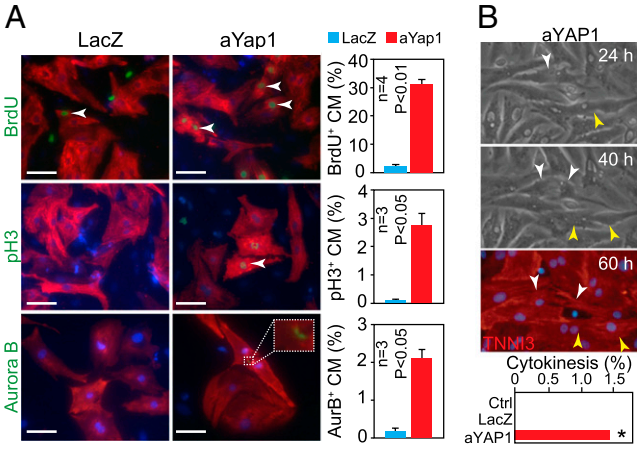

Fig. 3. Activated YAP1 stimulated proliferation of cultured cardiomyocytes. (*A*) aYAP1 stimulated cell-cycle activity of P4 neonatal rat cardiomyocytes, as measured by immunostaining for BrdU, pH3, and Aurora B (AurB). (Scale bars: 50 μm.) (*B*) Sequential imaging of cardiomyocytes at the indicated times after aYAP1 transduction. Two cardiomyocytes underwent cytokinesis in this field (arrowheads). At 60 h, cultures were immunostained for the cardiomyocyte marker TNNI3. Full imaging series is in Fig. S5*D*. *P = 0.015.

DEVELOPMENTAL BIOLOGY

fetal heart and control mice exposed to Dox starting at E8.5, as measured by the M-phase marker pH3 (Fig. 4 *C* and *D*). The S-phase marker EdU also increased by twofold, which approached, but did not achieve, statistical significance ($P = 0.07$, $n = 3$; Fig. 4 *B* and *D*). Thus, *Yap1* gain of function in fetal heart was sufficient to enhance cardiomyocyte proliferation, causing marked cardiomyocyte hyperplasia.

In control heart, the proliferation rate of cardiomyocytes was substantially lower in trabecular compared with compact myocardium (Fig. 4 *B* and *C*), indicating that, even in fetal heart, cardiomyocytes in specific compartments are exiting the cell cycle. This finding was particularly evident by pH3 staining, where it was very rare to observe $pH3^+$ trabecular cardiomyocytes. In contrast, proliferating mutant trabecular cardiomyocytes were readily observed in $Yap1^{GOF}$ (Fig. 4 *B* and *C*). Quantitation of EdU uptake showed that $Yap1^{GOF}$ stimulated trabecular myocardial proliferation fivefold, to levels comparable with compact myocardium (Fig. 4*E*). These data indicate that *Yap1* gain of function is sufficient to sustain cell-cycle activity in trabecular cardiomyocytes, causing tremendous expansion of trabecular myocardium.

Cardiomyocyte proliferation is often linked to differentiation. Trabecular and compact cardiomyocytes have distinct gene expression programs. One marker expressed in trabecular, but not compact, myocardium is *Nppa*. In situ hybridization showed that *Nppa* expression was strongly down-regulated in trabecular myocardium expressing activated YAP1 (Fig. S6*D*), consistent with impaired activation of the trabecular myocardial gene program.

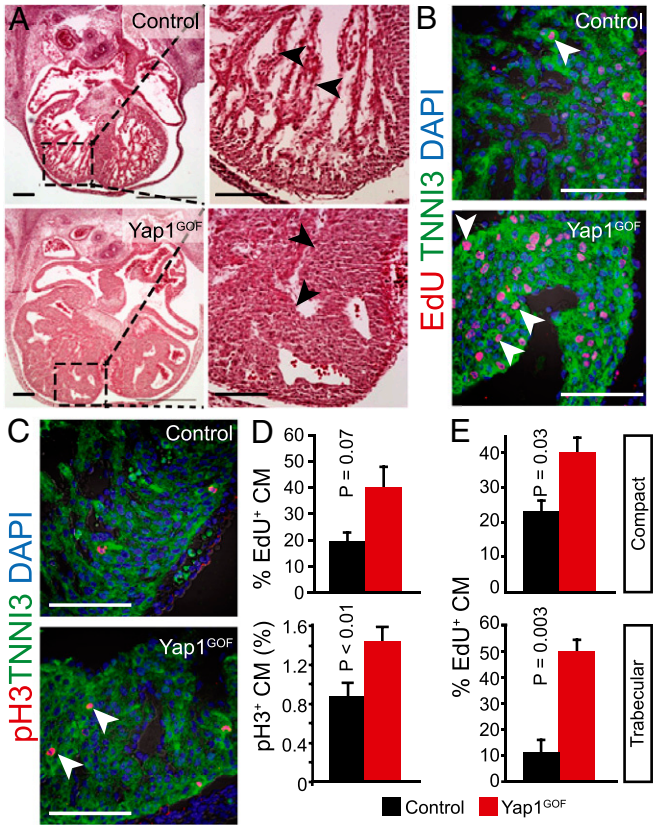

Fig. 4. Fetal YAP1 gain of function stimulated cardiomyocyte proliferation in vivo. (*A*) Histological sections of $Yap1^{GOF}$ heart at E12.5 revealed marked hypertrabeculation that nearly obliterated the cardiac chambers. Black arrowheads indicate trabecular myocardium. (*B* and *C*) pH3 and EdU staining showed elevated cardiomyocyte proliferation, particularly in trabecular myocardium (white arrowheads). (*D*) Quantitation of *B* and *C* for ventricular myocardium (compact and trabecular pooled). (*E*) Quantitation of cardiomyocyte EdU uptake in compact vs. trabecular myocardium. (Scale bars: 100 μm.)

Activated YAP1 Stimulated Postnatal Cardiomyocyte Proliferation in Vivo. In both P4 neonatal cardiomyocytes and fetal trabecular cardiomyocytes, YAP1 gain of function was sufficient to drive proliferation of cardiomyocytes that normally have exited the cell cycle. Therefore, we asked whether YAP1 gain of function was sufficient to drive proliferation of cardiomyocytes in the intact infant heart, in which cardiomyocytes are normally exiting from the cell cycle. We treated $Yap1^{GOF}$ mice with Dox from P5 and analyzed hearts at P15. Heart weight was increased in $YAP1^{GOF}$ mice compared with the controls (heart weight/body weight, 9.0 ± 0.1 vs. 7.5 ± 0.5 mg/g; $P = 0.03$; $n = 3$). This result was not due to cardiomyocyte hypertrophy, because cardiomyocyte size did not differ significantly between $Yap1^{GOF}$ and control groups (Fig. 5*A*). EdU labeling index was increased nearly twofold in $YAP1^{GOF}$ cardiomyocytes, indicative of a higher fraction of cardiomyocytes passing through S phase during the 24-h EdU pulse (Fig. 5*B*). This finding was corroborated by staining for the M-phase marker pH3, which showed 15-fold increased cell-cycle activity in $Yap1^{GOF}$ cardiomyocytes (Fig. 5*C*). Collectively, these data indicate that YAP1 gain of function increased postnatal cardiomyocyte proliferation.

YAP1 Regulates Expression of Cell-Cycle Genes in Cardiomyocytes. To begin to identify genes downstream of *Yap1* that stimulate cardiomyocyte proliferation, we performed microarray expression profiling in *Yap1* gain of function. We used the Affymetrix Rat Gene 1.0 ST microarray to compare gene expression between P4 neonatal cardiomyocyte transduced with FLAG-aYap1 or LacZ (control). Gene Set Enrichment Analysis (19) of the expression profiles using gene sets for manually curated canonical pathways indicated that the large majority of the sets significantly enriched by activated YAP1 related to cell proliferation and DNA synthesis (Fig. S7 *A* and *B*). Hierarchical clustering using cell cycle-related genes clustered samples into control or aYAP1 groups (Fig. 6*A* and Fig. S7*C*). Comparison of individual gene expression levels between groups identified 1,263 differentially expressed probe sets corresponding to 1,057 known genes ($n = 4$; $P < 0.005$ and fold change >50%; Dataset S1). We validated differential expression of a subset of cell cycle-regulated genes by qRT-PCR. Of eight genes tested that were differentially expressed by

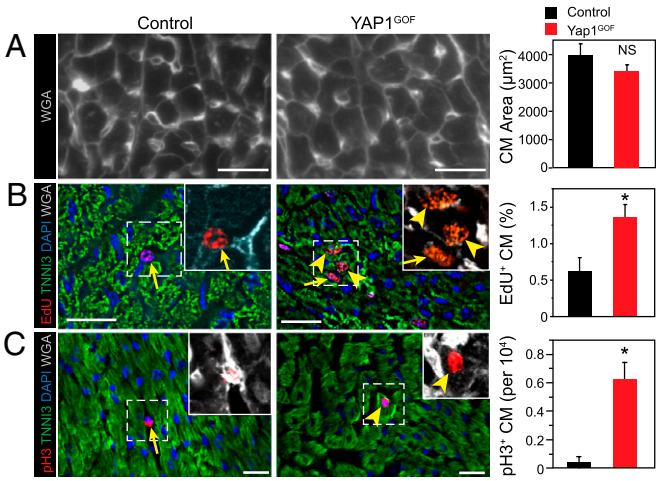

Fig. 5. Postnatal YAP1 gain of function stimulated cardiomyocyte proliferation in vivo. $YAP1^{GOF}$ or control mice were treated with Dox from P5 to P15, when they were analyzed for cardiomyocyte proliferation. (*A*) The size of YAP1 gain-of-function cardiomyocytes was indistinguishable from control. Wheat germ agglutinin (WGA) staining outlined the edges of cardiomyocytes. (*B* and *C*) Cardiomyocyte proliferation was increased based on EdU labeling index (*B*, deconvolution) and pH3 staining (*C*, confocal). Arrowheads indicate cardiomyocytes and arrows nonmyocytes. *Insets* show magnifications of boxed regions, with cardiomyocyte borders highlighted by WGA staining. $n = 3$. $^*P < 0.05$. (Scale bars: 20 μm.)

microarray, six were validated by qRT-PCR (Fig. 6*B*). Among up-regulated cell-cycle genes were Cyclin A2 (*CcnA2*), Cyclin B1 (*CcnB1*), and Cyclin-dependent kinase 1 (*Cdc2*), which have been shown to be sufficient to drive limited cardiomyocyte proliferation in postnatal hearts (20–22). Cyclins D1 and D2, which also promote cardiomyocyte proliferation (23, 24), approached but did not reach our cutoff thresholds for differential expression by microarray (P = 0.003–0.004 and fold change 1.4–1.5). These data indicate that YAP1 stimulates cardiomyocyte proliferation through the coordinate activation of a number of cell-cycle genes.

YAP1 Stimulation of Cardiomyocyte Proliferation Requires TEAD Interaction. In many contexts, coactivator YAP1 binds to TEAD family factors to stimulate cell proliferation (2). However, in some cases YAP1 regulation of cell growth is independent of TEAD factors (8). To assess the role of YAP1–TEAD interactions in promoting cardiomyocyte proliferation, we expressed GFP fused to a region of YAP1 sufficient to bind TEAD (25). We reasoned that this peptide, corresponding to amino acid residues 47–155 of YAP1, would interfere with YAP1–TEAD interaction (Fig. 7*A*) and named the peptide YTIP (YAP1–TEAD Interfering Peptide). In coimmunoprecipitation experiments, we confirmed that GFP–YTIP impaired YAP1–TEAD1 interaction (Fig. 7*B*).

We next measured the effect of GFP–YTIP on activated YAP1 stimulation of cardiomyocyte proliferation. GFP–YTIP strongly attenuated the stimulatory effect of activated YAP1 on proliferation of P4 neonatal cardiomyocytes, as measured by BrdU uptake and pH3 immunoreactivity (Fig. 7*C*). The antiproliferative effect of GFP–YTIP was paralleled by decreased activation of cell-cycle genes *Cdk1* and *Cyclin A2* by aYAP1 (Fig. 7*D*). These data indicate that YAP1 mitogenic activity in cardiomyocytes requires YAP1–TEAD interaction.

Substitution of YAP1 serine 79 by alanine selectively abolished TEAD interaction, and a $Yap1^{S79A}$ allele was unable to restore proliferation defects caused by ablation of wild-type Yap1 (11). We generated $Yap1^{fl/S79A}$::Tnnt2–Cre embryos, in which only the mutant, and not the wild-type, YAP1 protein would be expressed in the heart. These mutant mice exhibited cardiomyocyte hypoplasia at least comparable in severity to that caused by cardiomyocyte Yap1 ablation (Fig. 7*E*). These data indicate that YAP1 stimulation of cardiomyocyte proliferation requires TEAD interaction, both in vitro and in vivo.

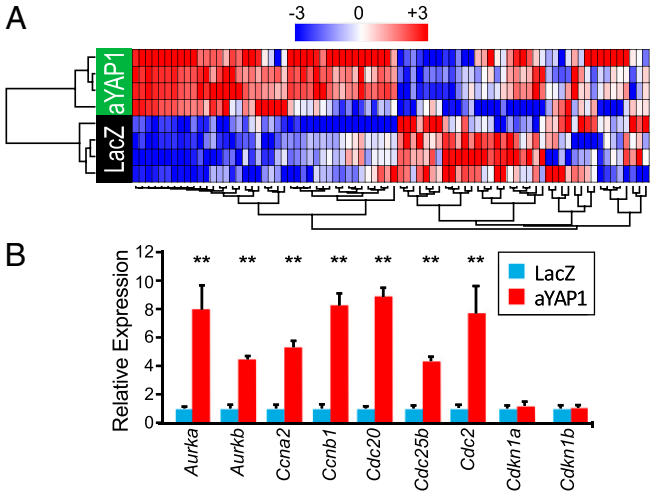

Fig. 6. YAP1 promotes expression of cell-cycle genes through interaction with TEAD1. (*A*) Heat map displaying two-way hierarchical clustering of cell-cycle genes in P4 neonatal cardiomyocytes expressing either aYAP1 or LacZ (control). Expression of cell-cycle genes segregated samples into treatment groups. (*B*) Validation of differential expression of cell-cycle genes by qRT-PCR. $^{**}P < 0.001$. $n = 4$.

Discussion

Growth of the mammalian heart occurs through both cardiomyocyte proliferation and hypertrophy, with proliferation and hypertrophy primarily driving fetal and postnatal heart growth, respectively. YAP1 has been shown to promote cellular proliferation and organ growth in multiple systems in flies and mammals (2). Although YAP1 regulation of organ growth through control of cellular proliferation has been studied in depth, little has been reported about YAP1 regulation of hypertrophic organ growth. Our results indicate that YAP1 is both necessary and sufficient for fetal cardiomyocyte proliferation. However, YAP1 is neither necessary nor sufficient for postnatal hypertrophic growth of the heart. Thus, our data indicate that YAP1 regulates organ size predominantly by controlling cell number.

Normal heart development requires precisely regulated regional heart growth. Selective hypoplasia of heart structures are seen in congenital heart disease such as hypoplastic left heart syndrome. Our study showed that proper regulation of YAP1 activity is critical for normal growth of the fetal heart. Interestingly, overall size of the left ventricular chamber was more severely affected in some $YAP1^{TNT}$ loss-of-function mutants (e.g., Fig. 1*C* and Fig. S3*D*). Moreover, it is likely that YAP1 activity is regionally controlled, so that localized disruption of YAP1 regulation could lead to selective chamber hypoplasia. Thus, mutation of genes in the YAP pathway may participate in pathogenesis of congenital heart disease involving abnormalities of myocardial growth.

Myocardial trabeculation is essential for fetal heart growth and function. Cardiomyocytes in trabeculae exit the cell cycle through unknown mechanisms, suggesting that growth of trabeculae occurs from addition of cardiomyocytes from compact myocardium. Neuregulin signaling to ErbB2/ErbB4 is essential for myocardial trabeculation (26, 27), and recent studies suggest that ErbB2 acts by promoting compact myocardial proliferation and directional cardiomyocyte migration into trabeculae (28). Our data indicate that

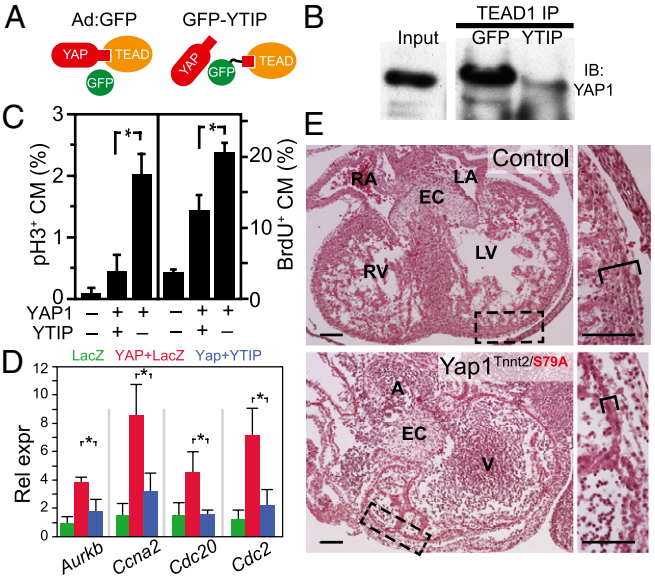

Fig. 7. YAP1 stimulation of cardiomyocyte proliferation requires TEAD interaction. (*A*) YAP1-TEAD inhibitory peptide (YTIP) strategy. (*B*) Endogenous TEAD1 and YAP1 interaction was blocked by Ad:GFP–YTIP in MES13 cells. (*C*) aYAP1 stimulation of P4 neonatal cardiomyocyte proliferation was attenuated by GFP–YTIP, as measured by BrdU and pH3 immunostaining. $^{*}P < 0.01$. $n = 3$. (*D*) Inhibition of TEAD interaction reduced expression of YAP1-activated cell-cycle genes, as measured by qRT-PCR. $^{*}P < 0.05$. $n = 3$. (*E*) Cardiomyocyte $YAP1^{S79A}$, deficient in TEAD interaction, did not support normal fetal myocardial growth. $Yap1^{Tnnt2/S79A}$ indicates the genotype $Yap1^{fl/S79A}$::Tnnt2–Cre. H&E-stained sections of E12.5 heart are shown. (*Right*) Boxed areas are enlarged. Brackets indicate compact myocardial thickness. (Scale bars: 100 μm.)

YAP1 is essential for regulating myocardial trabeculation, because trabeculation was reduced in YAP1^{TNT} mutants. This reduction of trabeculation may be a consequence of reduced proliferation of cardiomyocytes in compact myocardium. YAP1 activation in cardiomyocytes prevented trabecular cardiomyocyte cell-cycle exit, suggesting that negative regulation of the YAP1 pathway is essential for limiting trabecular myocardial expansion. Interestingly, YAP1 activation also prevented expression of the trabecular cardiomyocyte marker *Nppa*, suggesting that YAP1-induced trabecular proliferation is linked to impaired differentiation. Abnormalities of YAP1 regulation may contribute to myocardial noncompaction, which is seen in some forms of human cardiomyopathy.

The Hippo pathway is the best-known regulator of YAP1 activity. However, these kinases have multiple downstream targets and influence diverse processes such as apoptosis and autophagy (29). Indeed, the roles of Hippo pathway kinases LATS and MST in regulating these later processes have been explored by cardiomyocyte-restricted transgenic gain and inhibition of function (30, 31). Recently, cardiac-restricted inactivation of the Hippo pathway components *Sav1*, *Lats2*, or *Mst1/2* was shown to cause cardiac overgrowth (32). Thus, the findings of that study combined with those of the present study indicate that Hippo kinases restrain the proliferative activity of YAP1 on fetal cardiomyocytes.

Gene expression profiling showed that activated YAP1 potently and coordinately activated gene programs that promote cell-cycle activity. YAP1 activates transcription by binding to DNA-binding transcription factors, with TEAD1-4, orthologs of *Drosophila Scalloped*, being the best known (2). However, not all proliferative activities of YAP1 or its *Drosophila* ortholog Yorkie are mediated by TEAD/Scalloped. For example, *Yorkie* but not *Scalloped*, is required for growth of *Drosophila* imaginal discs (8). Using a dominant negative peptide that blocks YAP1–TEAD and a YAP1 point mutation-defective TEAD interaction, we showed that YAP1 stimulation of cardiomyocyte proliferation requires its interaction with TEAD.

Activated YAP1 potently promoted proliferation of fetal trabecular and neonatal ventricular cardiomyocytes that normally exit the cell cycle. These data show that activation of YAP1 can overcome signals that normally lead cardiomyocytes to exit the cell cycle. However, a limitation of the current study is that we cannot distinguish whether YAP1 is preventing cell-cycle withdrawal or reinitiating cell-cycle reentry. This limitation will need to be addressed further to test the hypothesis that activated YAP1 can induce cell-cycle reentry in adult, fully mature cardiomyocytes, with important potential ramifications for regenerative approaches to heart injury.

Materials and Methods

Please see *SI Materials and Methods* for details.

All animal procedures were approved by the Children's Hospital Boston Institutional Animal Care and Use Committee. TetO-YAP1 (10), Yap1^{flox} (11), Yap1^{S79A} (11), Rosa26^{mTmG} (15), Rosa26$^{fs\text{-}rtTA}$ (33), and Tnnt2-Cre (13) alleles were described.

Tnnt2–Cre adenovirus was constructed using the rat Tnnt2 promoter (34) and the AdEasy system (Stratagene). 3xFlag–YAP1 adenovirus expressed S127A-mutated human YAP1 cDNA with an N-terminal triple FLAG epitope tag. The GFP–YTIP construct contained eGFP fused to residues 47–155 of human YAP1. Cesium chloride gradient-purified viruses were titered with the AdEasy titer kit (Stratagene). Retro-orbital adenoviral injection to neonatal pups was performed as described (17).

Fetal and neonatal rat cardiomyocyte culture was performed by using the Neomyts cardiomyocyte dissociation kit (Cellutron). Adult cardiomyocytes were isolated by antegrade collagenase perfusion and purified by differential centrifugation.

Antibody sources are listed in Table S1. Primers for quantitative RT-PCR are in Table S2. Total RNA was isolated by using the RNeasy kit (Qiagen) and hybridized to Affymetrix microarrays (Rat Gene 1.0 ST).

Results are expressed as mean ± SEM. Two group comparisons were performed using Student *t* test.

ACKNOWLEDGMENTS. This work was supported by National Heart, Lung, and Blood Institute Grants HL095712 and HL100401 and by charitable contributions from Gail Federici Smith, Edward Marram, and Karen Carpenter.

1. Ishiwata T, Nakazawa M, Pu WT, Tevosian SG, Izumo S (2003) Developmental changes in ventricular diastolic function correlate with changes in ventricular myoarchitecture in normal mouse embryos. *Circ Res* 93:857–865.
2. Pan D (2010) The hippo signaling pathway in development and cancer. *Dev Cell* 19:491–505.
3. Zhao B, Lei QY, Guan KL (2008) The Hippo-YAP pathway: New connections between regulation of organ size and cancer. *Curr Opin Cell Biol* 20:638–646.
4. Harvey KF, Pfleger CM, Hariharan IK (2003) The Drosophila Mst ortholog, hippo, restricts growth and cell proliferation and promotes apoptosis. *Cell* 114:457–467.
5. Lai ZC, et al. (2005) Control of cell proliferation and apoptosis by mob as tumor suppressor, mats. *Cell* 120:675–685.
6. Pantalacci S, Tapon N, Léopold P (2003) The Salvador partner Hippo promotes apoptosis and cell-cycle exit in Drosophila. *Nat Cell Biol* 5:921–927.
7. Wu S, Huang J, Dong J, Pan D (2003) hippo encodes a Ste-20 family protein kinase that restricts cell proliferation and promotes apoptosis in conjunction with salvador and warts. *Cell* 114:445–456.
8. Wu S, Liu Y, Zheng Y, Dong J, Pan D (2008) The TEAD/TEF family protein Scalloped mediates transcriptional output of the Hippo growth-regulatory pathway. *Dev Cell* 14:388–398.
9. Zhang L, et al. (2008) The TEAD/TEF family of transcription factor Scalloped mediates Hippo signaling in organ size control. *Dev Cell* 14:377–387.
10. Camargo FD, et al. (2007) YAP1 increases organ size and expands undifferentiated progenitor cells. *Curr Biol* 17:2054–2060.
11. Schlegelmilch K, et al. (2011) Yap1 acts downstream of α-catenin to control epidermal proliferation. *Cell* 144:782–795.
12. Dong J, et al. (2007) Elucidation of a universal size-control mechanism in Drosophila and mammals. *Cell* 130:1120–1133.
13. Jiao K, et al. (2003) An essential role of Bmp4 in the atrioventricular septation of the mouse heart. *Genes Dev* 17:2362–2367.
14. Halder G, Johnson RL (2011) Hippo signaling: Growth control and beyond. *Development* 138:9–22.
15. Muzumdar MD, Tasic B, Miyamichi K, Li L, Luo L (2007) A global double-fluorescent Cre reporter mouse. *Genesis* 45:593–605.
16. Li F, Wang X, Capasso JM, Gerdes AM (1996) Rapid transition of cardiac myocytes from hyperplasia to hypertrophy during postnatal development. *J Mol Cell Cardiol* 28:1737–1746.
17. Jerome LA, Papaioannou VE (2001) DiGeorge syndrome phenotype in mice mutant for the T-box gene, Tbx1. *Nat Genet* 27:286–291.
18. Zhao B, et al. (2007) Inactivation of YAP oncoprotein by the Hippo pathway is involved in cell contact inhibition and tissue growth control. *Genes Dev* 21:2747–2761.
19. Subramanian A, et al. (2005) Gene set enrichment analysis: A knowledge-based approach for interpreting genome-wide expression profiles. *Proc Natl Acad Sci USA* 102:15545–15550.
20. Chaudhry HW, et al. (2004) Cyclin A2 mediates cardiomyocyte mitosis in the postmitotic myocardium. *J Biol Chem* 279:35858–35866.
21. Cheng RK, et al. (2007) Cyclin A2 induces cardiac regeneration after myocardial infarction and prevents heart failure. *Circ Res* 100:1741–1748.
22. Bicknell KA, Coxon CH, Brooks G (2004) Forced expression of the cyclin B1-CDC2 complex induces proliferation in adult rat cardiomyocytes. *Biochem J* 382:411–416.
23. Pasumarthi KB, Nakajima H, Nakajima HO, Soonpaa MH, Field LJ (2005) Targeted expression of cyclin D2 results in cardiomyocyte DNA synthesis and infarct regression in transgenic mice. *Circ Res* 96:110–118.
24. Soonpaa MH, et al. (1997) Cyclin D1 overexpression promotes cardiomyocyte DNA synthesis and multinucleation in transgenic mice. *J Clin Invest* 99:2644–2654.
25. Vassilev A, Kaneko KJ, Shu H, Zhao Y, DePamphilis ML (2001) TEAD/TEF transcription factors utilize the activation domain of YAP65, a Src/Yes-associated protein localized in the cytoplasm. *Genes Dev* 15:1229–1241.
26. Lee KF, et al. (1995) Requirement for neuregulin receptor erbB2 in neural and cardiac development. *Nature* 378:394–398.
27. Meyer D, Birchmeier C (1995) Multiple essential functions of neuregulin in development. *Nature* 378:386–390.
28. Liu J, et al. (2010) A dual role for ErbB2 signaling in cardiac trabeculation. *Development* 137:3867–3875.
29. Radu M, Chernoff J (2009) The DeMSTification of mammalian Ste20 kinases. *Curr Biol* 19:R421–R425.
30. Yamamoto S, et al. (2003) Activation of Mst1 causes dilated cardiomyopathy by stimulating apoptosis without compensatory ventricular myocyte hypertrophy. *J Clin Invest* 111:1463–1474.
31. Matsui Y, et al. (2008) Lats2 is a negative regulator of myocyte size in the heart. *Circ Res* 103:1309–1318.
32. Heallen T, et al. (2011) Hippo pathway inhibits Wnt signaling to restrain cardiomyocyte proliferation and heart size. *Science* 332:458–461.
33. Belteki G, et al. (2005) Conditional and inducible transgene expression in mice through the combinatorial use of Cre-mediated recombination and tetracycline induction. *Nucleic Acids Res* 33:e51.
34. Wang G, Yeh HI, Lin JJ (1994) Characterization of cis-regulating elements and trans-activating factors of the rat cardiac troponin T gene. *J Biol Chem* 269:30595–30603.

Supporting Information

von Gise et al. 10.1073/pnas.1116136109

SI Materials and Methods

Mice. All animal procedures were approved by the Institutional Animal Care and Use Committee. Col-TetO-YAP1 (1), Yap1^{flox} (2), Yap1^{S79A} (2), Rosa26^{mTmG} (3), Rosa26$^{fs\text{-}rtTA}$ (4), and Tnnt2–Cre (5) alleles were described. Dox was administered to pregnant dams at 1 mg/mL in drinking water. For delivery to lactating pups, Dox in maternal drinking water was supplemented with IP injection of 100 μg per g of body weight daily. Gestational age was determined by checking for vaginal plugs, with noon of the day of the plug defined as E0.5. Ascending aortic constriction was performed as described (6).

Adenoviruses. Tnnt2-Cre adenovirus was constructed using the rat Tnnt2 promoter (7) and the AdEasy system (Stratagene). 3xFlag–YAP1 adenovirus was generated by cloning S127A-mutated human YAP1 cDNA with an N-terminal triple FLAG epitope tag into pENTR3C (Invitrogen). The GFP–YTIP construct was generated by cloning eGFP, a 15-amino acid C-terminal linker, and residues 47–155 of human YAP1 into pENTR3C. These expression cassettes were then transferred to pAd/CMV/V5-DEST by using LR clonase (Invitrogen). Viruses were purified on cesium chloride gradients and titered by using the AdEasy adenoviral titer kit (Stratagene). Retro-orbital adenoviral injection to neonatal pups was performed as described (8).

Cardiomyocyte Isolation and Culture. Fetal and neonatal rat cardiomyocyte culture was performed by using the Neomyts cardiomyocyte dissociation kit (Cellutron). Cardiomyocytes were enriched by preplating on tissue culture plastic to remove nonmyocytes. P4 neonatal cardiomyocytes were initially cultured for 48 h in the presence of 20 μM cytosine B-D-arabinofuranoside(araC; Sigma) and 5% (vol/vol) horse serum to prevent proliferation of nonmyocytes. Then cardiomyocytes were transduced with virus (multiplicity of infection, 25) in serum-free medium and cultured for an additional 48 h. For BrdU labeling, we treated cells for 24 h with 10 μM BrdU. Cells were fixed with 4% (wt/vol) PFA and immunostained. For quantitation of cardiomyocyte number, cells were cultured on labeled, gridded dishes (MatTeK) and sequentially imaged. Adult cardiomyocytes were isolated by antegrade collagenase perfusion and purified by differential centrifugation.

Histology. H&E staining was performed on paraffin-embedded sections. Immunostaining was performed on cryosections and detected with Alexa-labeled secondary antibodies (Invitrogen). Antibody sources are listed in Table S1. EdU was administered intraperitoneally at 200 μg (pregnant dams) or 5 μg per g of body weight (pups), 2 or 24 h before tissue collection, respectively. EdU was detected with Click-iT chemistry (Invitrogen). Imaging was performed on a Nikon TE2000 epifluorescent microscope with deconvolution (Volocity; Perkin-Elmer) or on an Olympus FV1000 confocal.

Gene Expression. Western blotting was performed by using specific antibodies (Table S1). Total RNA was isolated by using the RNeasy kit (Qiagen) and hybridized to Affymetrix microarrays (Rat Gene 1.0 ST). Array data were deposited at the Gene Expression Omnibus (GEO) database (accession no. GSE33019). For qRT-PCR, RNA was reverse transcribed (Superscript III) and specific transcripts were measured by using Sybr Green chemistry and normalized to GAPDH. Primer sequences are provided in Table S2.

1. Camargo FD, et al. (2007) YAP1 increases organ size and expands undifferentiated progenitor cells. *Curr Biol* 17:2054–2060.
2. Schlegelmilch K, et al. (2011) Yap1 acts downstream of α-catenin to control epidermal proliferation. *Cell* 144:782–795.
3. Muzumdar MD, Tasic B, Miyamichi K, Li L, Luo L (2007) A global double-fluorescent Cre reporter mouse. *Genesis* 45:593–605.
4. Belteki G, et al. (2005) Conditional and inducible transgene expression in mice through the combinatorial use of Cre-mediated recombination and tetracycline induction. *Nucleic Acids Res* 33:e51.
5. Jiao K, et al. (2003) An essential role of Bmp4 in the atrioventricular septation of the mouse heart. *Genes Dev* 17:2362–2367.
6. Bisping E, et al. (2006) Gata4 is required for maintenance of postnatal cardiac function and protection from pressure overload-induced heart failure. *Proc Natl Acad Sci USA* 103:14471–14476.
7. Wang G, Yeh HI, Lin JJ (1994) Characterization of cis-regulating elements and trans-activating factors of the rat cardiac troponin T gene. *J Biol Chem* 269:30595–30603.
8. Jerome LA, Papaioannou VE (2001) DiGeorge syndrome phenotype in mice mutant for the T-box gene, Tbx1. *Nat Genet* 27:286–291.

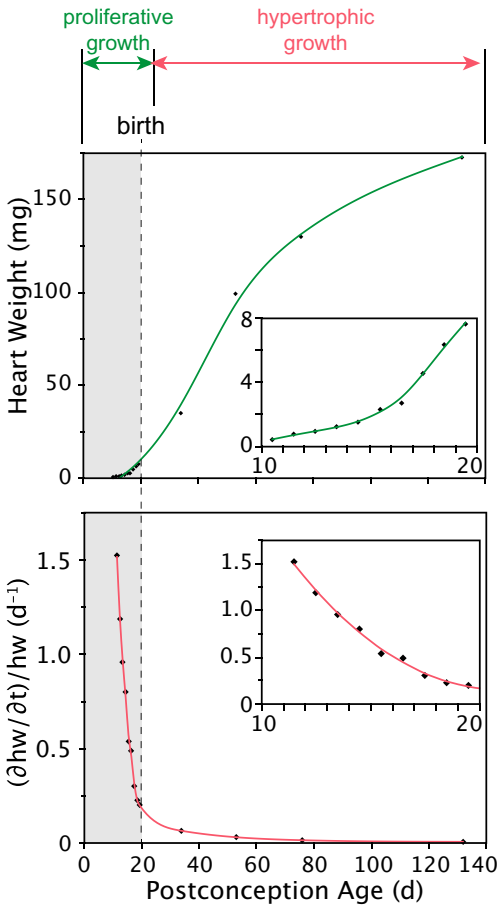

Fig. S1. Growth of the mammalian heart. Fetal growth occurs through cardiomyocyte proliferation, and postnatal growth occurs through cardiomyocyte hypertrophy. The fold increase in heart weight between E10.5 and birth and birth to adulthood is comparable. The rate of change of heart weight normalized to the size of the heart, a measure of the growth velocity at the cellular level, decreases rapidly with increasing age.

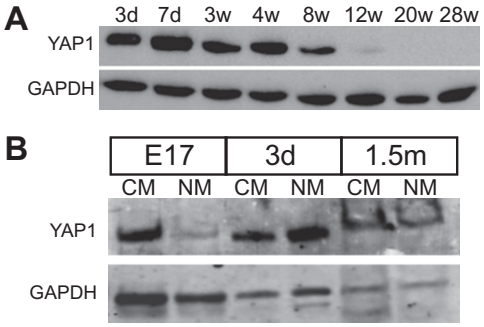

Fig. S2. Cardiac YAP1 expression. (*A*) Postnatal YAP1 expression in myocardium. Postnatal age is indicated. d, days; w, weeks. (*B*) YAP1 expression in cardiomyocytes (CM) and nonmyocytes (NM) at indicated developmental stages. Myocardium was dissociated by collagenase digestion, and the cardiomyocyte fraction was isolated by differential plating (fetal and neonatal) or differential centrifugation (adult). E, embryonic.

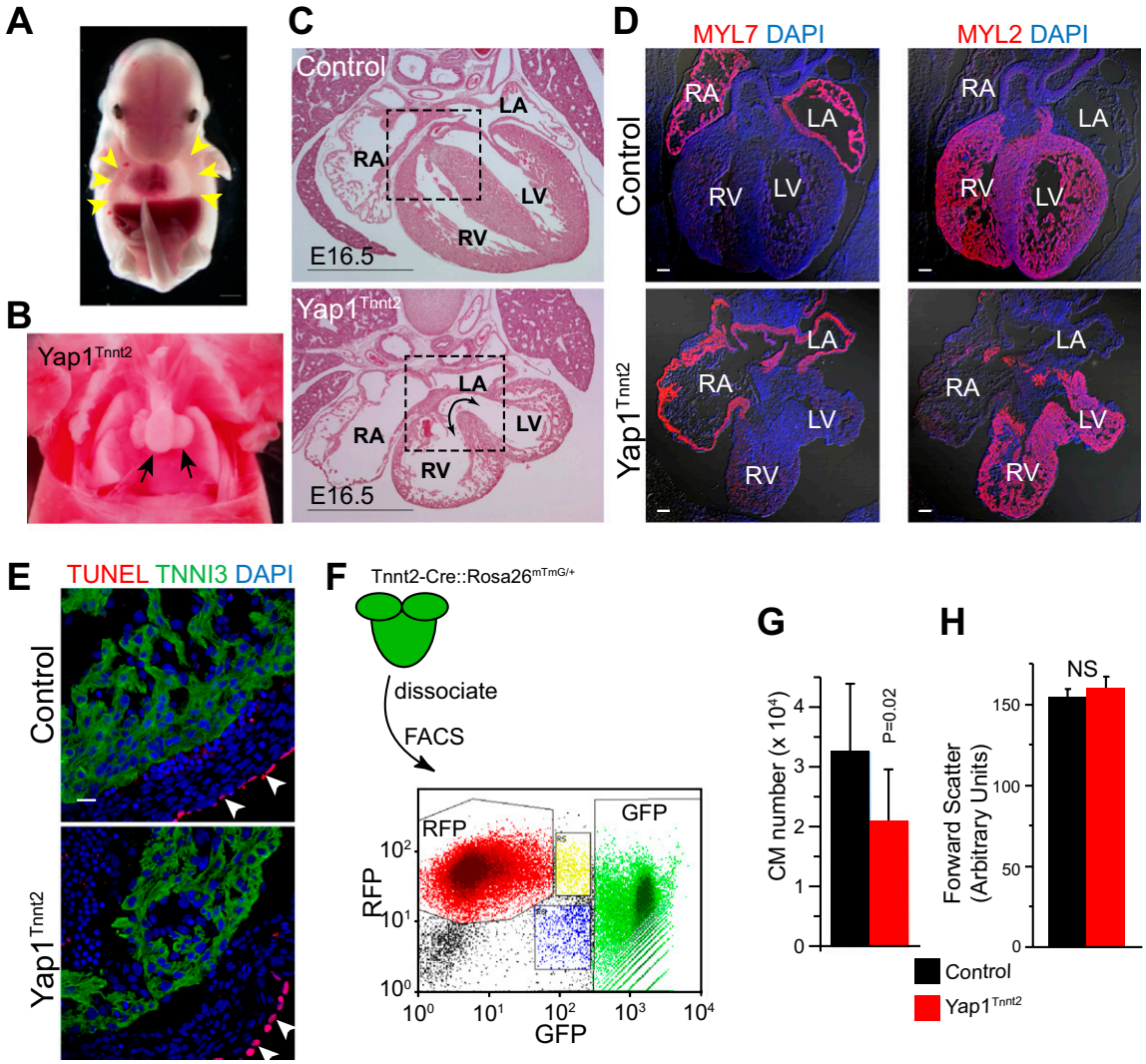

Fig. S3. Histological and FACS analysis of Yap1-deficient fetal hearts. (*A*) Whole-mount view of backlit embryo showing translucent mutant chest (arrowheads) due to pericardial effusion. (*B*) Example of a mutant heart with severe global myocardial hypoplasia. Overall cardiac patterning was preserved. Lungs shape was normal despite cardiac hypoplasia. (*C*) Membranous VSD in a rare Yap1^{Tnnt2} mutant that survived to E16.5. (*D*) Expression of chamber-specific markers MYL2 and MYL7 was unchanged in Yap1-deficient hearts. (Scale bars: 100 μm.) (*E*) TUNEL staining indicated no significant change in apoptosis rate in Yap1^{Tnnt2} heart. Arrowheads indicate apoptotic nuclei in skin. (Scale bar: 10 μm.) (*F*) FACS analysis of fetal cardiomyocytes, isolated by sorting for Tnnt2-Cre activated expression of mGFP from the Rosa26^{mTmG} allele. (*G*) Total cardiomyocyte number was reduced in Yap1^{Tnnt2} mutant heart compared with control. n = 9–11. (*H*) Cell size, as estimated by forward scatter, was unchanged between control and YAP1-deficient cardiomyocytes. n = 9–11.

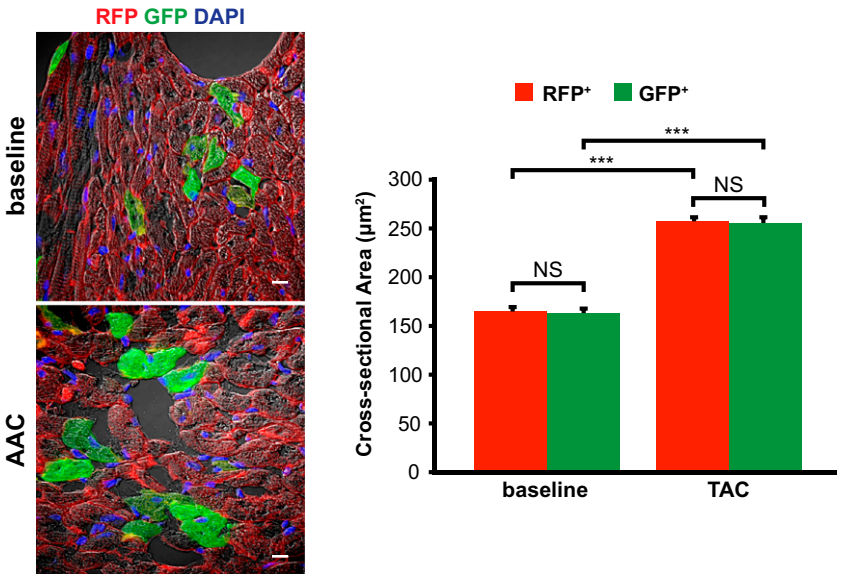

Fig. S4. YAP1 is not required for pathological cardiac hypertrophy. Mice with mosaic cardiac YAP1 inactivation were treated with ascending aortic constriction (AAC) or no operation at 6 wk. One week later, cardiomyocyte cross-sectional areas were measured. GFP^+ (YAP1-depleted) and RFP^+ (control) cardiomyocyte cross-sectional areas were not statistically different (NS). More than 280 cardiomyocytes were measured per group. ***$P < 0.001$. (Scale bars: 10 μm.)

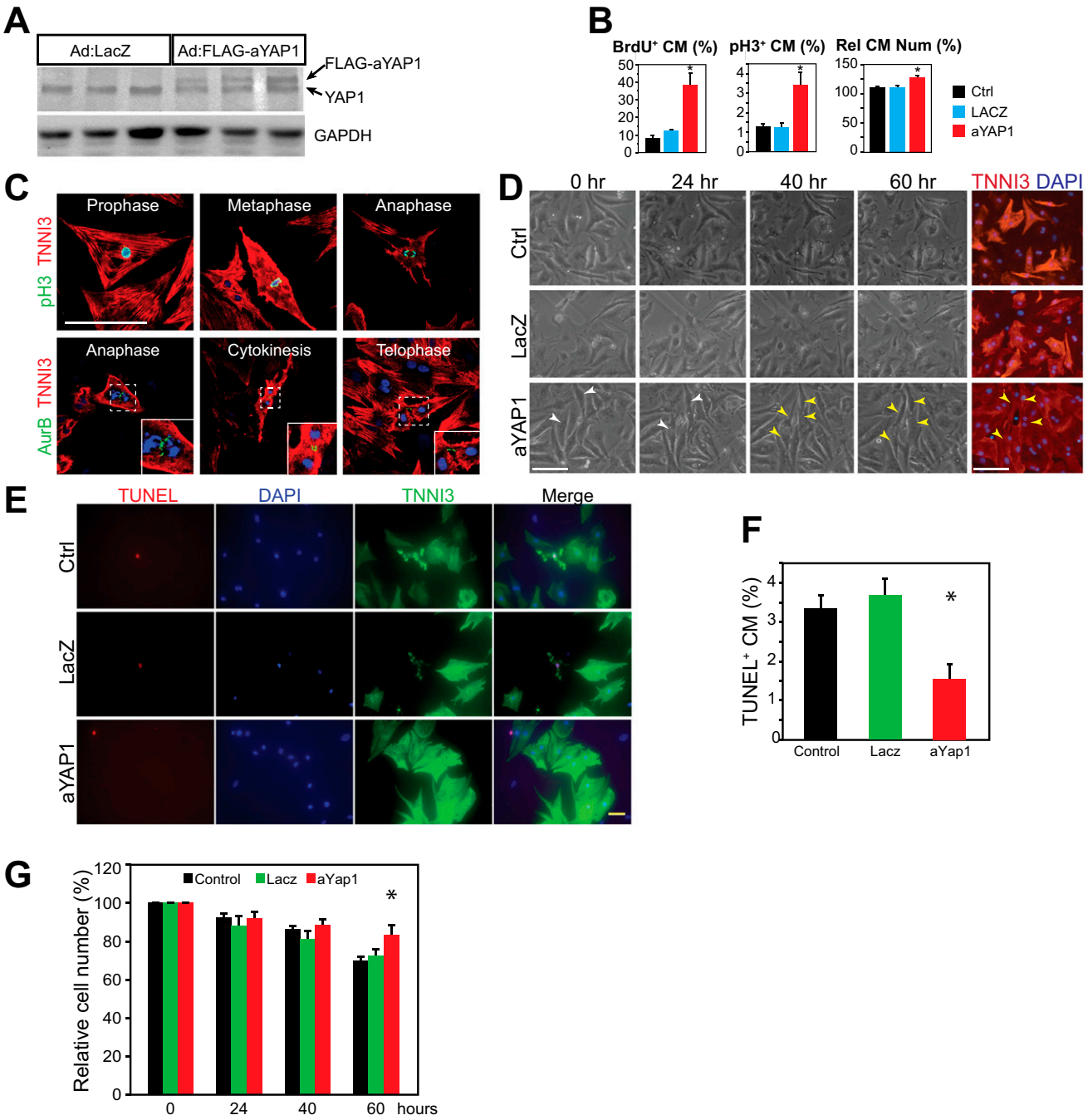

Fig. S5. Activated YAP1 stimulated proliferation of cultured fetal and postnatal cardiomyocytes. (*A*) Adenoviral expression of activated YAP1 (aYAP1) in neonatal rat cardiomyocytes. YAP1 was detected with specific antibody. (*B*) aYAP1 stimulated proliferation of E16.5 fetal rat cardiomyocytes. $n = 3$. $^*P < 0.05$. (*C*) Different phases of mitosis induced by expression of aYAP1. Red, TNNI3. (Scale bar: 50 μm.) (*D*) Serial observation of cardiomyocyte division. P4 NRVMs were plated on gridded tissue culture dishes and observed sequentially for cytokinesis. Times indicate hours after virus treatment. White arrows indicate cardiomyocytes undergoing cytokinesis. Yellow arrowheads indicate cardiomyocytes just after cytokinesis. TNNI3 staining was performed on fixed cells after the culture period to confirm lineage identity. Cardiomyocyte cytokinesis was not observed in untreated (control) or LacZ adenovirus-treated groups. (Scale bars: 50 μm.) (*E*) A subset of P4 NRVMs underwent apoptosis during the culture period, as indicated by TUNEL staining. (Scale bar: 20 μm.) (*F*) aYAP1 reduced apoptosis of cultured cardiomyocytes. (*G*) Quantitation of absolute cell number by sequential imaging indicated that cardiomyocyte number declined during the culture period. Cardiomyocyte number declined least in the aYAP1 group. $^*P < 0.05$ vs. LacZ.

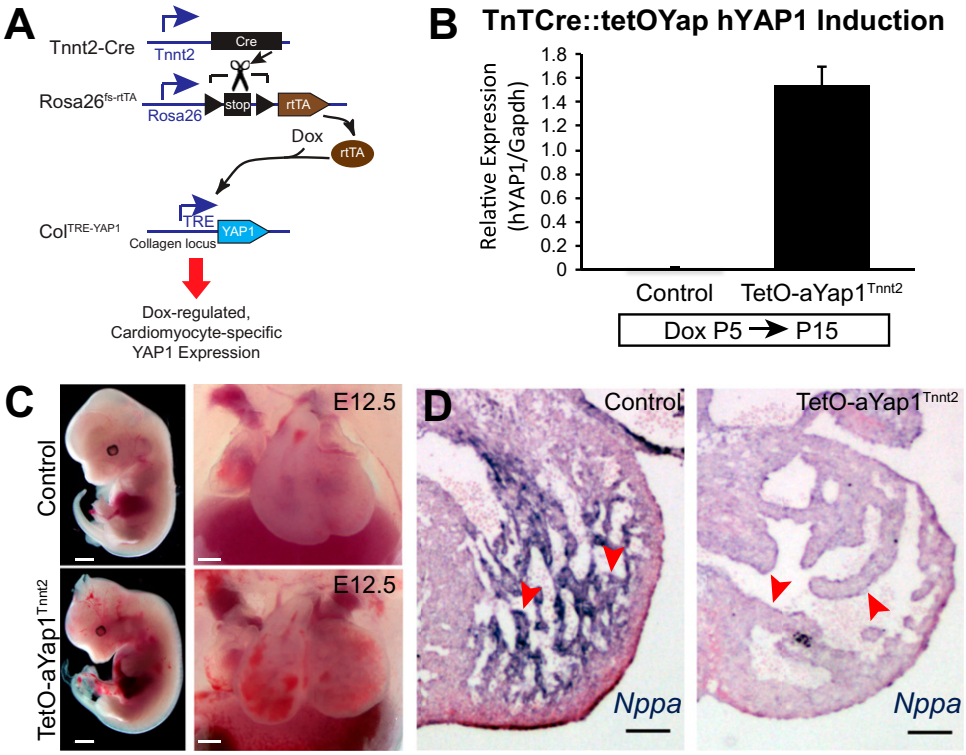

Fig. S6. Fetal YAP1 gain of function stimulated cardiomyocyte proliferation in vivo. (*A*) Genetic strategy for cardiomyocyte-restricted YAP1 gain of function. Tnnt2–Cre recombination of Rosa26$^{fs-rtTA}$ resulted in cardiomyocyte-restricted expression of the rtTA, which stimulated activated human YAP1 expression from a Dox-regulated promoter positioned distal to the collagen locus. (*B*) Induction of the human YAP1 transgene by Dox. qRTPCR was performed with primers specific for human YAP1. (*C*) Peripheral hemorrhage and growth retardation of mutant embryo at E12.5. Hearts of mutant embryos were enlarged and exhibited pockets of pooled blood. (Left bars: 1 mm; right bars: 250 μm.) (*D*) Nppa in situ hybridization of E12.5 left ventricle. Trabecular myocardium (red arrowheads) expressed markedly lower *Nppa* transcript levels in TetO-aYap1^{Tnnt2} compared with control. (Scale bars: 100 μm.)

A

Rank	Name	Size	FDR (q-val)
1	Reactome Mitotic Prometaphase	77	0.000
2	Reactiome Cell Cycle Mitotic	262	0.000
3	Reactome Mitotic M M G1 Phases	132	0.000
4	Reactome G2 M Transition	72	0.000
5	Reactome Cetrosome Matruation	60	0.000
6	Reactome Loss of NLP from Mitotic Centrosomes	53	0.000
7	Kegg Cell Cycle	106	0.002
8	Reactome Cholesterol Biosynthesis	20	0.009
9	Reactome G2 M Checkpoints	34	0.010
10	Reactome Inactivation of APC Via Direct Inhibition of the AP Complex	15	0.029
11	Kegg Steroid Biosynthesis	16	0.027
12	Biocarta ATBRCA Pathway	18	0.030
13	Kegg Homologous Recombination	24	0.033
14	Reactome Activation of the PRE Replicative Complex	21	0.032
15	Reactome Double Strand Break Repair	20	0.035
16	Biocarta Cell Cycle Pathway	19	0.033
17	Reactome E2F-Mediated Regulation of DNA Replication	22	0.042
18	Reactome Mitochondrial tRNA Aminoacylation	17	0.048

B

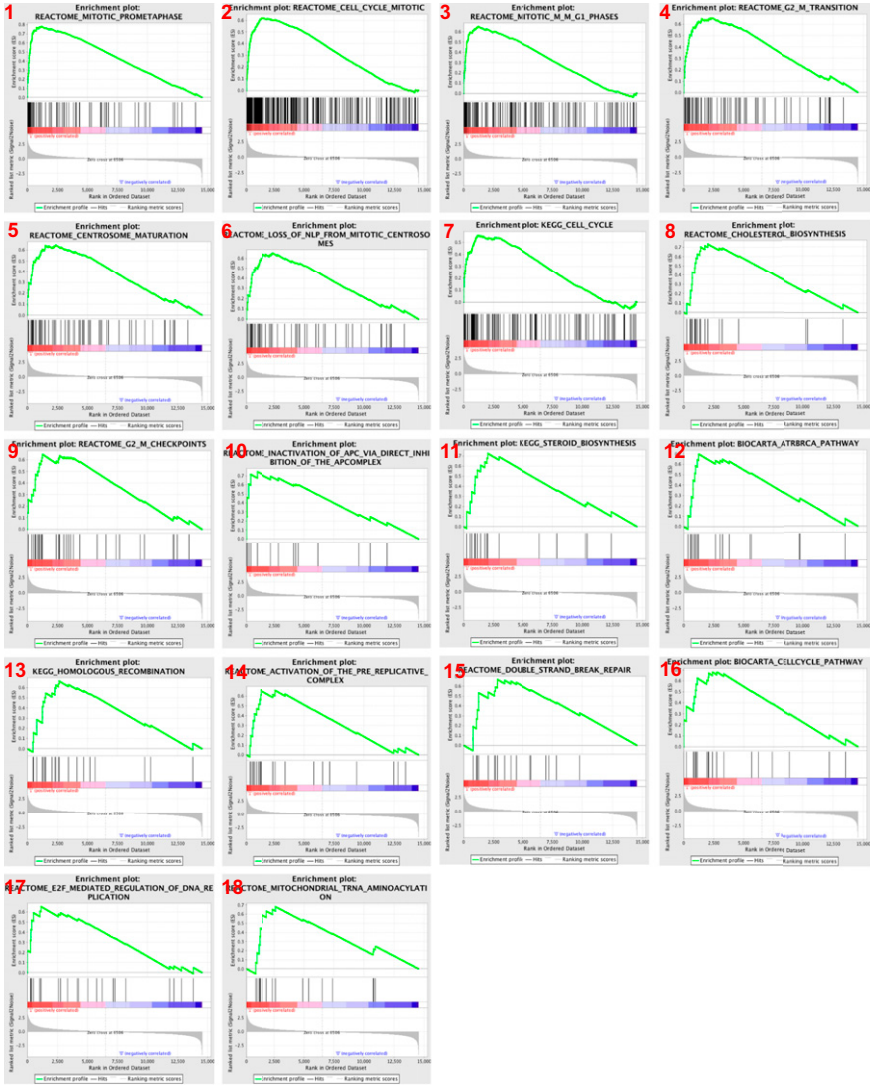

C

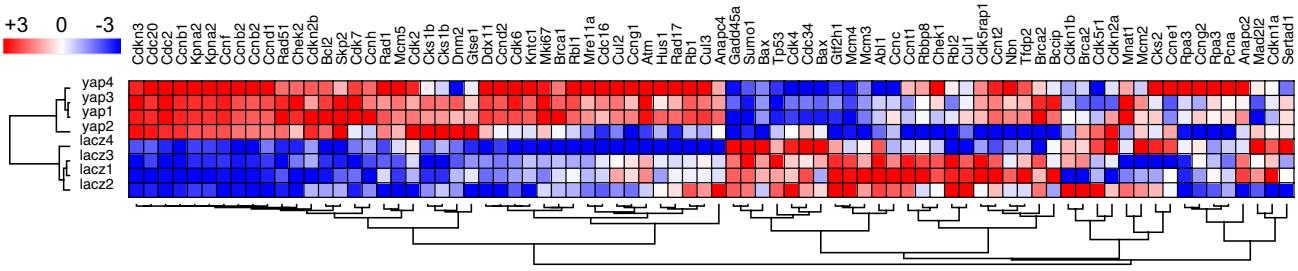

Fig. S7. YAP1 promotes expression of cell-cycle genes. (*A* and *B*) Gene Set Enrichment Analysis was performed by using gene expression profiles of P4 NRVMs expressing activated YAP1 or control (LacZ) on curated canonical pathway gene sets. (*A*) Gene sets significantly enriched (FDR < 0.05) in activated YAP1 expressing NRVMs. (*B*) Enrichment graphs showing overrepresentation of indicated gene set members among genes more highly expressed in activated YAP1 compared with control. Red numbers correspond to ranks indicated in *A*. (*C*) Heat map displaying two-way hierarchical clustering of cell cycle genes in P4 NRVMs expressing either aYAP1 or LacZ (control). Expression of cell-cycle genes clustered samples into treatment groups. This is the same heat map as in Fig. 6*A* but in expanded form with gene symbols.

Table S1. Antibodies and other staining reagents used in this study

Antibody/staining reagent	Supplier	Catalog no.
Aurora B	Abcam	ab2254
BrdU	Abcam	Ab6326
EdU	Invitrogen	C10338
GAPDH	Sigma	G8795
MYL2	Sigma	AT10493
MYL7	Santa Cruz	sc66967
pH3	Millipore	06-570
TEAD1	BD	610923
TNNI3 (cardiac Troponin I)	Abcam	ab56357
TUNEL	Roche	12 156 792 910
WGA, AlexaFluor 647 conjugate	Invitrogen	W32466
YAP1	Sigma	Y4770
Digoxigenin-AP	Roche	11 093 274 910

Table S2. qRT-PCR primers used in this study

Gene	Forward primer	Reverse primer
Aurka	GGGTGGTCTGTGCATGCTCCG	GCCTCAAAAGGAGGCATCCCCACTA
Aurkb	ATGAGCAGCGGACTGCCACG	GTCCAGGGTGCCGCACATGG
Ccna2	CCCGGAGCCAGAAAACCACTGGT	GTCCACAAGGATGGCCCGCAT
Ccnb1	TGCGAACCAGAGGTGGAACTGGA	TTCCATTGGGCTTGGAGAGGGAGT
Cdc20	GGCTGGGTTCCCCTGCAGACAT	TGGGCAAAGCCATGGCCTGAGA
Cdc25b	TGGTGGCCCTGTTGACAGGC	GCGGCACATCCGTGGTCCAC
Cdc2	TTTCGGCCTTGCCAGAGCGTT	GTGGAGTAGCGAGCCGAGCC
Cdkn1a	ATGTACCAGCCACAGGCACCATG	GGGACCGAACAGACGACGGC
Cdkn1b	GGCCTTCGACGCCAGACGTAA	GCGCAATGCTACATCCAATGCTT
YAP1	ABI assay Mm00494240_m1	
GAPDH	ABE assay 4352339E	
Yap S127A	AGCTGCTGGGCCAGAGACTACT	TCGAGCTCATGCCTCTCCAGC

Other Supporting Information Files

Dataset S1 (XLS)